Bol. Soc. Paran. Mat.
©SPM – E-ISSN-2175-1188
SPM: www.spm.uem.br/bspm

(3s.) **v. 2026 (44) 12** : 1–12.
ISSN-0037-8712
doi:10.5269/bspm.81571

Squeeze Film Couplestress Lubrication Rendered with a Porous Layer in a Sphere-to-Sphere Configuration - An Analytical Study

Divya R., Sreekala C. K., Hanumagowda B. N., Pramod S.

ABSTRACT: The paper aims to study the role of non- Newtonian couple stresses fluid and porous media on the squeeze film characteristics by considering a sphere-to-sphere geometry. The modified Reynolds equation for the geometry is derived, incorporating the non-Newtonian effects of couple stress fluids and porosity. Closed-form expressions for essential squeeze film characteristics are obtained, including pressure distribution, load-carrying capacity, and squeeze film time. It is observed that as the couple stress parameter value increases, the pressure, load-carrying capacity, and squeeze time also increase. Furthermore, the squeeze film pressure, load, and squeezing time increase with an increase in the radius ratio. Conversely, the introduction of porosity results in lower pressure, load, and squeezing time. These results provide significant insights into the efficacy of bearing lubrication when it is used in porous environments with couple stress fluids.

Keywords: Sphere-to-sphere configuration, couple stress fluid, radius ratio, porous, film thickness.

Contents

1. Introduction

The squeeze-film mechanism is commonly applied in both machinery and human physiology. Within engineering applications, it enables bearings to support loads at reduced speeds and is utilised in accelerometers, gyroscopes and MEMS to manage vibrations. It also plays an important role in dampers used in turbines and rotating machines to minimise vibrations. In the field of biomechanics, fluids present in joints like synovial fluid act as natural lubricants, enabling friction reduction, absorbing shock loads and protecting against wear. The same concept is applied in shock absorbers, wet clutches, and seals to maintain smooth functioning and improve their lifespan.

The study of squeeze film lubrication has been fundamental to tribology, beginning with the seminal work of Reynolds [1] , who is responsible for deriving the traditional hydrodynamic lubrication theory for Newtonian fluids using thin-film conditions. Early analytical work, of Hays' [2] variational formulation for rectangular plates, contributed valuable theory on finite geometries, pressure fields, and load-carrying behaviour on parameters such as film thickness and curvature. However, such traditional formulations applied to Newtonian fluids and omitted inertial and viscoelastic influences, which restricts relevance to modern lubricants and biofluids. With progress in computational tools, researchers started to study non-Newtonian fluid properties. Phan-Thien et al. [3] analysed viscoelastic fluids and found that the stress overshoot improves load -bearing capacity and influences transient film characteristics. Couple-stress fluid model, derived from Stokes' [4] microcontinuum framework, expanded classical lubrication theory by including particle-size influences and additional velocity gradients, introducing a characteristic length parameter to describe non-Newtonian rheology. According to Lin's [5,6] analyses of couple-stress fluid, improved pressure fields, noticeable increase in load capacity and reduced surface approach of the surfaces in finite journal bearing and in sphere-plate systems are demonstrated, whereas Bujurke Jayaraman [7] demonstrated the significance of couple stresses in describing lubrication in synovial joints. Furthermore, Lin [8] - [10] expanded the scope of systems altered by inertial forces, each demonstrating that couple

2020 *Mathematics Subject Classification:* 76A10, 76D08.
Submitted January 27, 2026. Published April 21, 2026.

stresses accentuate film rigidity, improve damping, and increase load supporting capability. Recently, Lin [11] examined the fusion of ferrofluids into couple-stress models, which has demonstrated synergistic enhancements, where applied magnetic fields further increase load support and extend film durability.

Porous media, which enable fluid flow through interconnected cavities, play a crucial role in machine bearings, physiological joints, and various thermal applications. Recent investigations have integrated the characteristics of couple-stress fluids and porous media to formulate more representative models for modern tribological and biomedical technologies, which has brought another dimension to squeeze film research, Naduvinamani et al. [12,13] analysed short as well as elongated porous journal bearings and demonstrated that couple-stress enhances load supporting capability and squeezing duration, while permeability weakens these gains. Later, Poroelastic models proposed by Nabhani et al. [14,15] incorporated Darcy-Brinkman-Forchheimer relations, unifying shear viscosity, inertia, and elastic-matrix, which expanded the analysis to support cartilage-like domains. Roughness introduced by Bujurke [16] shows that polar additives and surface roughness with couple stresses enhances load supporting capacity, and squeeze time, whereas permeability wanes these effects. Furthermore, Lin et al. [17] demonstrated that viscosity dependence and applied magnetic fields yield additional improvements in squeezing performance. Similarly, Vasanth et al. [18] examined these results for porous annular plates, whereas Kumar et al. [19] analysed circular plates showing that pressure-dependent viscosity and couple stress improve lubrication, whereas permeability wanes this enhancement. Several researchers have investigated squeeze-film lubrication by incorporating various physical effects—such as magnetohydrodynamics (MHD), slip-velocity conditions, and surface roughness—across a wide range of bearing geometries. For instance, Vinutha et al. [20,21] performed a theoretical analysis on the altogether impact of MHD, slip velocity, on rough triangular plates and on a long cylinder and infinite rough plate using couplestress fluid. Similarly, Kasinath and Upadhaya [22] studied the effects of roughness on a porous pivoted slider bearing with couple stress fluid lubrication. A comparative study between radial and azimuthal roughness is conducted between curved circular and porous rough flat plate by Salma et al. [23] using couple stress lubrication.

Sphere–sphere contact lubrication is relevant in several practical systems characterised by localised point contact and high contact pressures. Typical examples include ball bearings, where lubrication occurs between the rolling elements and the raceways; gear mechanisms such as bevel and hypoid gears; biomedical systems, particularly the articulation between the acetabulum and the femoral head in human synovial joints; shock absorbers and damping devices, where squeeze-film effects are significant; MEMS and NEMS components, including micro-switches and micro-bearings; and spherical joints and ball-and-socket mechanisms used in spacecraft and other aerospace applications. Existing research, such as the work by Lin et al. [24], indicates that couple stress fluids significantly influence squeeze film features between two spheres, particularly at lesser film heights and with greater radius ratios and couple-stress parameter values.

Noting the scarcity of research on squeeze-film dynamics in sphere-to-sphere setups, this article introduces a novel method to fill this void by exploring squeeze film couple stress lubrication between two spheres, where the lower sphere is porous. The integration of porosity within a sphere-to-sphere couple-stress framework has not been previously investigated in the literature. This study is driven by the recognition that incorporating porous media in couple stress lubrication is crucial for enhancing system performance, preventing early failure, and prolonging the lifespan of the bearing.

2. Mathematical Formulation

Figure 1 depicts the lubricant film configuration between a sphere-to-sphere geometry. The fixed cylindrical coordinate system is defined such that its origin lies at the midpoint of the minimum film thickness. The upper surface S_2 of radius R_2 is approaching with a squeeze velocity, $V_{sq} = -\frac{\partial h}{\partial t}$, to the lower fixed surface S_1, of radius R_1, which is rendered with a porous layer.

When $R_1, R_2 >> x$, the lubricant film thickness between the gap of the surfaces may be approximated by the parabolic expression proposed by Hamrock [25] as

$$h_1 = \frac{h_m}{2} + \frac{r^2}{2R_1} \tag{2.1a}$$

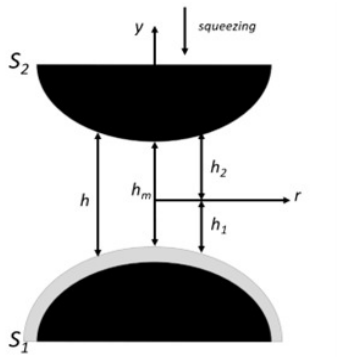

Figure 1: Geometrical illustration of the squeeze film lubrication between a sphere-to-sphere system

$$h_2 = \frac{h_m}{2} + \frac{r^2}{2R_2} \tag{2.1b}$$

where h_m represents the minimum film thickness along the central line, while h_1 and h_2 correspond to film thickness contributions from upper and lower surfaces evaluated from the horizontal $r\theta-$plane. Hence, the overall film thickness h, combining these contributions as reported by Lin et al. [24], is

$$h = h_1 + h_2 = h_m + \frac{(R_1 + R_2)}{2R_1R_2} r^2 \tag{2.2}$$

The lubricant present between the two spheres is considered to be an incompressible Stokes couple stress fluid. Assuming that body forces and body couples are negligible and the thin-film theory of lubrication by Pinkus and Sternlicht [26] is applicable, the continuity equation, together with equations of motion governing symmetric radial flow of couple stress fluid as formulated by Stokes [4] is

$$\mu \frac{\partial^2 u}{\partial y^2} - \eta \frac{\partial^4 u}{\partial y^4} = \frac{\partial p}{\partial r} \tag{2.3}$$

$$\frac{\partial p}{\partial y} = 0 \tag{2.4}$$

$$\frac{1}{r}\frac{\partial (ru)}{\partial r} + \frac{\partial v}{\partial y} = 0 \tag{2.5}$$

The flow velocities u^*, v^* in the porous matrix, as described by Darcy's law,

$$u^* = \frac{-k}{\mu(1-\phi)} \left(\frac{\partial p^*}{\partial r} \right) \tag{2.6}$$

$$v^* = \frac{-k}{\mu(1-\phi)} \left(\frac{\partial p^*}{\partial y} \right) \tag{2.7}$$

Where $\phi = \dfrac{\left(\frac{\eta}{\mu}\right)}{k}$ $\rightarrow$ ratio of characteristic microstructural length scale to the pore size, $\eta \rightarrow$ material constant characterising couple stress, $\mu \rightarrow$ viscosity coefficient, $k \rightarrow$ permeability of porous material. And for the porous region continuity equation becomes

$$\frac{1}{r}\frac{\partial (ru^*)}{\partial r} + \frac{\partial v^*}{\partial y} = 0 \tag{2.8}$$

Together with vanishing couplestresses and no-slip conditions, the boundary conditions for radial and axial components of velocity are

(i) At the upper surface, $y = h_2$:

$$u = 0, \quad v = -\frac{\partial h}{\partial t}, \quad \frac{\partial^2 u}{\partial y^2} = 0 \tag{2.9a}$$

(ii) At the lower surface, $y = -h_1$:

$$u = 0, \quad v = -v^*, \quad \frac{\partial^2 u}{\partial y^2} = 0 \tag{2.9b}$$

Using the boundary conditions (2.9a) & (2.9b), and solving equation (2.3) using equation (2.4), the radial velocity component obtained is

$$u = \frac{1}{2\mu}\frac{\partial p}{\partial r}\left[\left(2l^2 - h_1h_2 + y^2 + (h_1 - h_2)y\right) - 2l^2\left\{\frac{\cosh\left(\frac{2y + h_1 - h_2}{2l}\right)}{\cosh\left(\frac{h_1 + h_2}{2l}\right)}\right\}\right] \tag{2.10}$$

Where the couple stress parameter l is given by

$$l = \left(\frac{\eta}{\mu}\right)^{\frac{1}{2}} \tag{2.11}$$

Substituting (2.10) in (2.5) and solving using boundary conditions (2.9a) & (2.9b), we obtain the Modified Reynolds equation as

$$\frac{1}{r}\frac{\partial}{\partial r}\left[\frac{r}{\mu}\frac{\partial p}{\partial r}\, g(h, l)\right] = -12\,\frac{\partial h}{\partial t} \tag{2.12}$$

Where

$$g(h, l) = 24l^3 \tanh\left(\frac{h}{2l}\right) + \frac{12k\delta}{(1 - \phi)} - 12l^2h + h^3 \tag{2.13}$$

Non-dimensionalising using quantities

$$h_1^* = \frac{h_m^*}{2} + \frac{r^{*^2}}{2\alpha\beta}, \qquad h_2^* = \frac{h_m^*}{2} + \frac{r^{*^2}}{2\beta}, \qquad h_m^* = \frac{h_m}{h_{m0}},$$

$$r^* = r/R2$$

$$h^* = h_1^* + h_2^* = h_m^* + \frac{(\alpha + 1)}{2\alpha\beta}\, r^{*^2}, \qquad l^* = \frac{l}{h_{m0}}, \qquad \alpha = \frac{R_1}{R_2}, \qquad \beta = R_2h_{m0}, \quad \psi = \frac{k\delta}{h_{m0}^3}$$

We get the modified dimensionless Reynolds equation as ,

$$\frac{1}{r^*}\frac{\partial}{\partial r^*}\left\{g(h^*, l^*, \psi)\; r^*\,\frac{\partial p^*}{\partial r^*}\right\} = -\frac{12}{\beta} \tag{2.14}$$

Where,

$$g(h^*, l^*, \psi) = 24l^{*^3} \tanh\left(\frac{h^*}{2l^*}\right) + \frac{12\psi}{(1 - \phi)} - 12l^{*^2}h^* + h^{*^3} \tag{2.15}$$

In non-dimensional quantities, α represents the radius ratio, β indicates the initial film-radius, and l^* corresponds to the nondimensional couple-stress, while h_{m0} indicates the initial minimum film thickness between the two spheres.
The boundary conditions associated with non-dimensional film pressure are

$$\frac{\partial p^*}{\partial r^*} = 0, \qquad \text{at } r^* = 0,$$

$$p^* = 0, \qquad \text{at } r^* = 1$$

Integrating equation (2.14) twice w.r.to r^* and applying the specified boundary conditions, the expression for the squeeze film pressure exerted by the upper plate in closed form is

$$p^* = \frac{6}{\beta}\int_{r^*}^{1} \frac{r^*}{g(h^*,\, l^*,\, \psi)}\, dr^* \tag{2.16}$$

The load-carrying capacity is

$$W = 2\pi \int_{0}^{R_2} p\, r\, dr \tag{2.17}$$

Integrating equation (2.17) by making use of equation (2.16), the dimensionless load carrying capacity is

$$W^* = \frac{12\pi}{\beta}\int_{0}^{1}\left[\int_{r^*}^{1} \frac{r^*}{g(h^*,\, l^*,\, \psi)}\, dr^*\right] r^*\, dr^* \tag{2.18}$$

Based on the above expression, the dimensionalesss squeezing time is

$$t^* = \frac{W h_{m0}^2}{\mu R_2^4} = \frac{12\pi}{\beta}\int_{h_m^*}^{1}\left[\int_{0}^{1}\left\{\int_{r^*}^{1} \frac{r^*}{g(h^*,\, l^*,\, \psi)}\, dr^*\right\} r^*\, dr^*\right] dh_m^* \tag{2.19}$$

3. Results and Discussion

The impact of key physical parameters on the squeeze-film behaviour of a porous sphere-to-sphere geometry with couple-stress fluid as lubricant is examined. The key parameters considered include the minimum film thickness (h_m^*), porosity parameter(ψ), couple-stress parameter (l^*), and radius ratios (α) and initial film radius (β). Their influence on the dimensionless pressure distribution, load-carrying capacity, and response time is analysed and presented graphically.

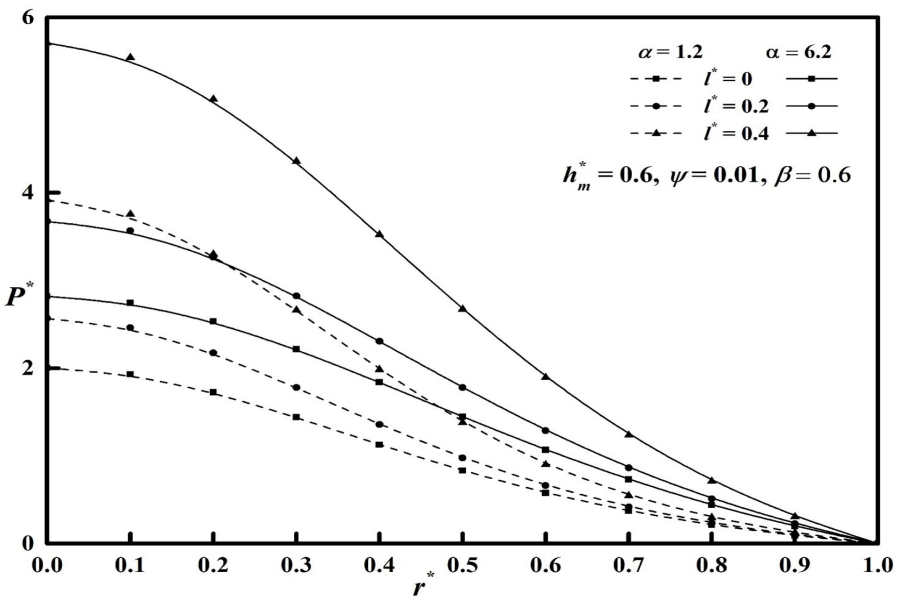

Figure 2: Dimensionless pressure P^* versus radial co-ordinate r^* for different couplestress (l^*) parameter values.

Figure 2 indicates the changes in dimensionless Pressure P^* against dimensionless radial coordinate r^* for distinct values of l^* at $\alpha = 1.2$ and 6.2. The results are evaluated taking $h_m^* = 0.6, \psi = 0.01$ and $\beta = 0.6$. Near the centre, the region around $r^* = 0$, the presence of couple stresses ($l^* = 0.2, 0.4$) is found to produce greater film pressure compared to the Newtonian lubricant case($l^* = 0$). This can be ascribed to the additional resistance offered by the microstructural effects inherent in the couple-stress fluids. Furthermore, increasing the radius ratio ($\alpha = 6.2$) leads to a greater conformity between spherical surfaces, resulting in a wider contact region and more fluid confined in the region offers an increased resistance to the squeezing motion. Moreover, the microstructural effects of couplestress fluids also enhance this resistance. Consequently, squeeze film pressure increases with the intensifying effects of couple-stress fluids and radius ratios.

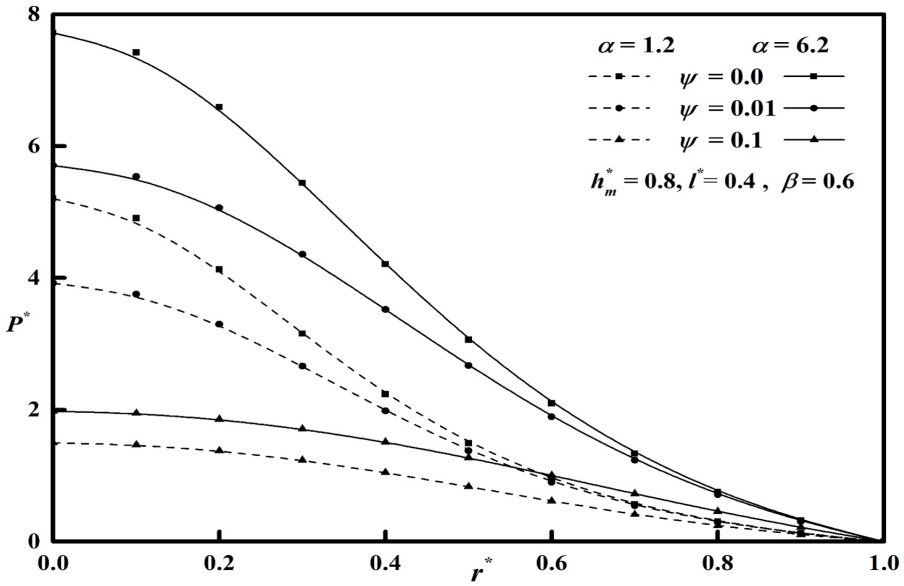

Figure 3: Dimensionless pressure P^* versus radial co-ordinate r^* for different different porosity ψ parameter values.

Figure 3 presents the distribution of dimensionless pressure P^* with dimensionless radial coordinate r^* for different values of porosity parameter ψ at radius ratios α=1.2 and 6.2. The results correspond to dimensionless minimum film height $h_m^* = 0.8$, couple stress parameter $l^* = 0.4$ and initial film radius $\beta = 0.6$. It is observed that near the central region around $r^* = 0$, the presence of porosity ($\psi = 0.01, 0.1$) leads to lower film pressure compared to a non-porous case ($\psi = 0.0$). This is due to the seepage of fluid into the porous matrix, which decreases fluid confinement and wanes the pressure buildup within the film. Furthermore, increasing the radius ratio ($\alpha = 6.2$) results in improved lubricant retention, thereby reducing the impact of porosity on the pressure distribution due to its larger conformity between spherical surfaces. As a result, the adverse effect of porosity on squeeze-film pressure is partially offset, and the pressure distribution becomes less sensitive to variations in the porosity parameter.

Figure 4 illustrates the changes in dimensionless load W^* against dimensionless minimum film height h_m^* for distinct values of l^*, at $\alpha = 1.2$, and 6.2, ψ=0.01 and β=0.6. It is viewed clearly that W^* decreases monotonically with an increase in h_m^*, which is consistent with the classical squeeze film behaviour. It is also examined that the presence of couple stresses ($l^* = 0.2, 0.4$) significantly intensifies the load carrying capability, especially in the region of smaller film thickness (Near the region around $h_m^* = 0.5$), compared to the Newtonian case ($l^* = 0.0$). Furthermore, increasing the radius ratio ($\alpha = 6.2$) also amplifies the impact of couple stresses on W^*. This increased load carrying capability can be attributed to enhanced pressure buildup due to microstructural and radius ratio effects, as explained in **Figure 2**.

Figure 5 illustrates the changes in dimensionless load W^* with dimensionless minimum film height h_m^* for distinct values of ψ at α=1.2 and 6.2, with l^*=0.4 and β=0.6. For all the cases, W^* decreases steadily

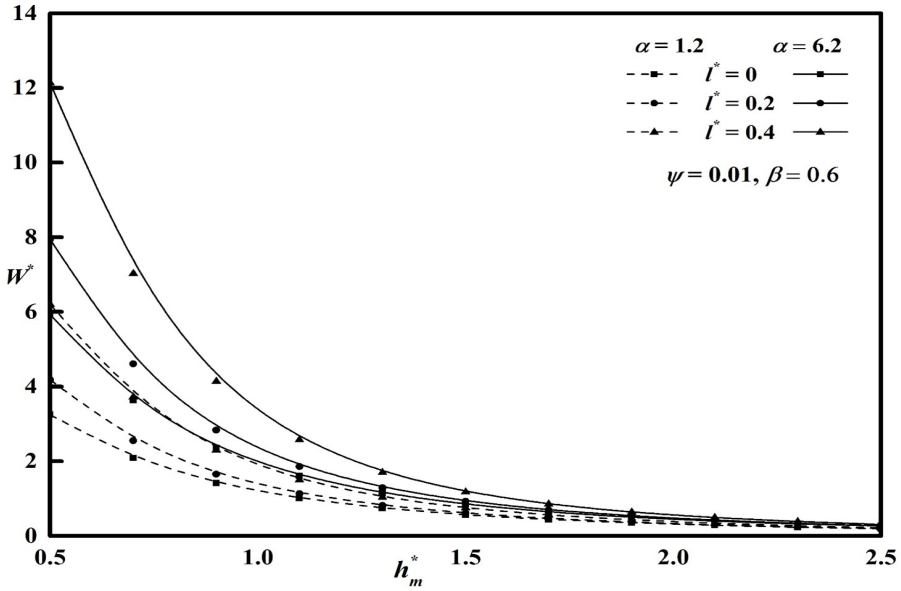

Figure 4: Dimensionless Load W^* versus h_m^* for different couplestress (l^*) parameter values.

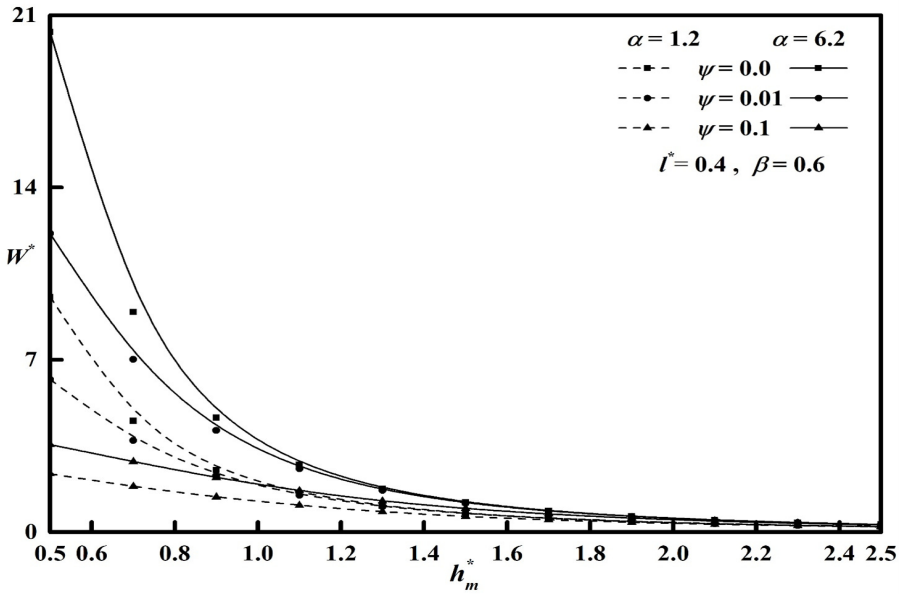

Figure 5: Dimensionless Load W^* versus h_m^* for distinct porosity ψ parameter values.

with an increase in h_m^* due to the decrease in squeeze film generation with increasing film thickness. The presence of porosity ($\psi = 0.01, 0.1$) is found to produce a lesser load-carrying capacity as lubricants seep into the porous surface, particularly at smaller film thickness. Moreover, higher radius ratios in combination with couplestress lubricant enhance load carrying capability even under porous conditions, especially in thin film regimes.

Figure 6 illustrates the changes in dimensionless squeezing time t^* with dimensionless squeeze film thickness h_f^* for different values of l^* at $\alpha = 1.2$ and 6.2, with ψ=0.01 and $\beta = 0.6$. For all the cases, it is viewed that squeezing time t^* decreases continuously with increasing h_f^*. Basically, when the film is thin,

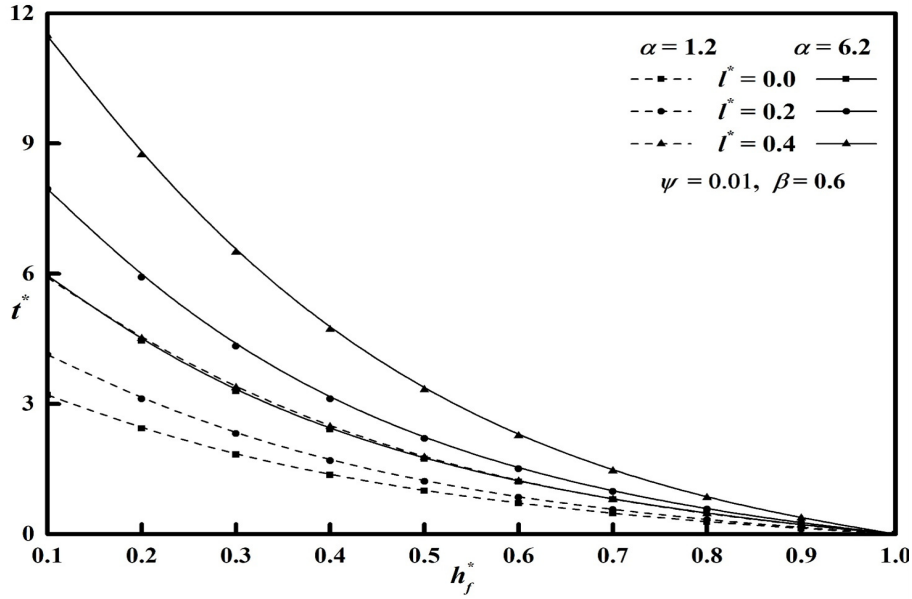

Figure 6: Dimensionless squeezing time t^* versus h_f^* for different couplestress (l^*) parameter values.

the squeezing process becomes slow due to the high resistance offered by the lubricant to the approaching surfaces. Moreover, couplestress fluids also offer resistance due to their microstructural effects. Hence, a larger time is required to squeeze the film out. Furthermore, larger radius ratios creates enlarged contact region, which intensifies the squeeze-film action and increases the time required for the lubricant to be expelled. Thus, a larger radius ratio, stronger couplestress effects and thin squeeze films are required to significantly prolong the squeezing time even when the surface is rendered porous.

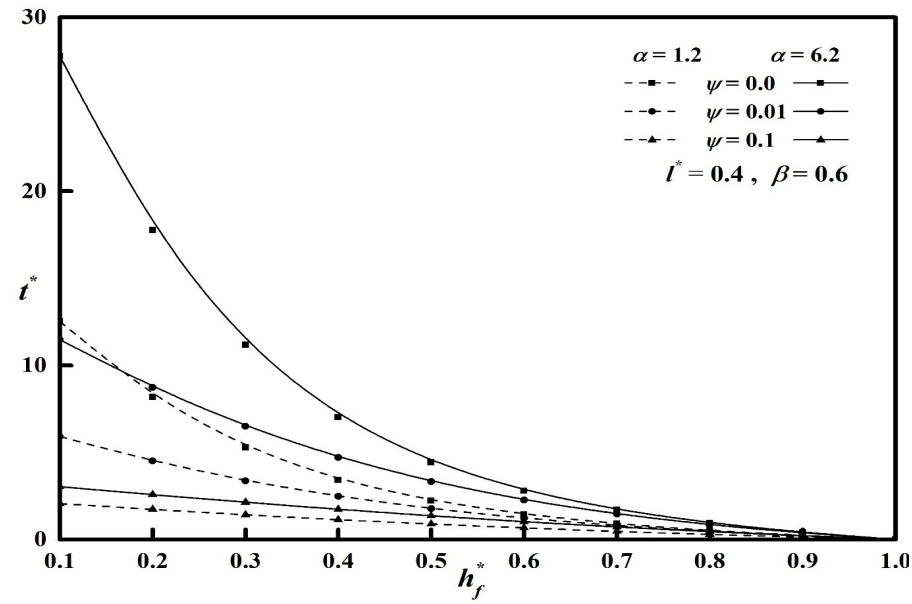

Figure 7: Dimensionless squeezing time t^* versus h_f^* for different porosity (ψ) parameter values.

Figure 7 illustrates the variation of dimensionless response time t^* with dimensionless squeeze film

thickness h_f^* for various values of ψ at $\alpha = 1.2$ and 6.2, $l^* = 0.4$ and $\beta = 0.6$. It indicates that dimensionless squeezing time t^* decreases monotonically with increasing squeeze film thickness h_f^* for all parameter values, indicating faster system response for thicker films. An increase in α significantly enhances t^*, especially in the thin-film region, whereas introducing porosity through parameter ψ and increasing its values reduces squeezing time due to the fluid retention in the porous region. Overall, the results highlight that couple-stress effects and radius ratios play a crucial role in prolonging squeeze time, especially under thin-film conditions, even in the presence of surface porosity.

Table 1 describes a numerical comparison between the present analysis and the results presented by Lin [24] when the system is a non-porous surface $\psi = 0$. An excellent agreement is observed for all values of the couple-stress parameter l^* and radius ratios $\alpha = 1$ and $\alpha = 5$, thereby validating the accuracy and correctness of the present formulation and numerical procedure. The table also includes results for a porous surface ($\psi = 0.01$), which are not available in Lin [24] literature. The presence of porosity leads to a noticeable reduction in the non-dimensional pressure, load-carrying capacity, and response time compared to the non-porous case. This reduction becomes more pronounced with increasing l^* and radius ratio α, reflecting the combined influence of surface porosity and couple-stress effects on the squeeze-film characteristics.

Table 1: Numerical comparison of the present analysis with those of Lin [24] for P^*, W^* and t^* with $r^* = 0.8$, $h_m^* = 0.3$, $h_f^* = 0.1$, $\beta = 0.6$

		Lin [24] Analysis		Present Analysis			
		$\alpha = 1$	$\alpha = 5$	$\psi = 0$		$\psi = 0.01$	
	l^*			$\alpha = 1$	$\alpha = 5$	$\alpha = 1$	$\alpha = 5$
P^*	0	0.183955	0.43403	0.183955	0.43403	0.181599	0.421392
	0.2	0.201641	0.505909	0.201641	0.505909	0.198796	0.488714
	0.4	0.252096	0.713112	0.252096	0.713112	0.247603	0.67901
W^*	0	6.76894	15.4916	6.76894	15.4916	4.86147	10.2963
	0.2	13.7299	34.2585	13.7299	34.2585	6.56448	14.4985
	0.4	34.4194	90.0864	34.4194	90.0864	9.60501	21.4566
t^*	0	6.09204	13.9425	6.09204	13.9425	4.37533	9.26667
	0.2	12.3569	30.8327	12.3569	30.8327	5.90803	13.0487
	0.4	30.9774	81.0778	30.9774	81.0778	8.6445	19.3109

The relative pressure R_P^*, relative load R_W^* and relative squeezing time R_t^* are evaluated using the expressions,

$$R_P^* = \frac{P^*_{\text{porous}} - P^*_{\text{non-porous}}}{P^*_{\text{porous}}} \times 100$$

$$R_W^* = \frac{W^*_{\text{porous}} - W^*_{\text{non-porous}}}{P^*_{\text{porous}}} \times 100$$

$$R_t^* = \frac{t^*_{\text{porous}} - t^*_{\text{non-porous}}}{P^*_{\text{porous}}} \times 100$$

Table 2 summarises the influence of porosity and couple-stress effects on the relative squeeze-film characteristics. The negative values of R_P^*, $R_W^*$and R_t^* indicate a reduction in pressure, load-carrying capacity, and squeezing time due to the presence of surface porosity compared to the non-porous case. It is visible that for a fixed l^*, an increase in ψ results in a substantial decrease in all three relative quantities due to the weak pressure build-up within the lubricant film, which consequently lowers the load support and response time due to the fluid seepage into the porous matrix. Furthermore, the reduction becomes more noticeable with increasing l^*. At higher values of the couple-stress parameter, the interaction between microstructural effects of the lubricant and porous surface characteristics increases,

leading to greater enhancement of squeeze-film performance. These results clearly indicate that although couple-stress fluids enhance squeeze-film behaviour, the presence of porosity significantly counteracts this enhancement.

Table 2: Nondimensional Relative Pressure R_P^*, Relative Load R_W^* and Relative squeezing time R_t^* with $r^* = 0.8, h_m^* = 0.3, h_f* = 0.1, \beta = 0.6$

l^*	ψ	R_P^*	R_W^*	R_t^*
0	0.001	-2.62888	-6.44607	-7.81567
	0.01	-20.5172	-33.5362	-37.5801
	0.1	-69.0711	-75.6536	-78.9145
0.2	0.001	-4.61005	-20.918	-23.9379
	0.01	-30.662	-57.6791	-61.283
	0.1	-78.1848	-87.5743	-89.4019
0.4	0.001	-10.0824	-41.5452	-45.2845
	0.01	-48.6314	-76.1822	-78.7457
	0.1	-88.015	-94.5012	-95.3997

4. Conclusions

Based on the Stokes micro-continuum theory, the influence of couple stresses and based on Darcy's law, the effects of porosity on the squeeze film characteristics between two distinct spheres have been investigated

- Compared with the corresponding Newtonian-lubricant case, the presence of couple stresses significantly enhances the maximum pressure, load-carrying capacity and squeezing time.
- Increasing the radius ratio of the spheres further amplifies the pressure, load-carrying capability and squeezing time, whereas increasing the porosity leads to a reduction in these squeeze film characteristics.
- Furthermore, the influence of couple stresses becomes more pronounced at smaller minimum film thicknesses and higher values of the couple-stress parameter and radius ratio.

These findings are particularly relevant for practical applications such as spherical bearings and biomedical joints, where delayed surface approach, improved load support and enhanced damping characteristics are desirable.

Acknowledgments

We think the referee by your suggestions.

References

1. O. Reynolds, On the theory of lubrication, Trans. R. Soc. Lond. 177 (1886) 157–234.
2. D.F. Hays, Squeeze films for rectangular plates, J. Basic Eng. 85 (2) (1963) 243–248.
3. N. Phan-Thien, F. Sugeng, R.I. Tanner, The squeeze-film flow of a viscoelastic fluid, J. Non-Newtonian Fluid Mech. 24 (1) (1987) 97–119.
4. V.K. Stokes, Couple stresses in fluids, Phys. Fluids 9 (1966) 1709–1715.
5. J.-R. Lin, Squeeze film characteristics of finite journal bearings: couple stress fluid model, Tribol. Int. 31 (4) (1998) 201–207.
6. J.-R. Lin, Squeeze film characteristics between a sphere and a flat plate: couple stress fluid model, Comput. Struct. 75 (1) (2000) 73–80. https://doi.org/10.1016/S0045-7949(99)00080-2.
7. N.M. Bujurke, G. Jayaraman, Influence of couple stresses in squeeze films, Int. J. Mech. Sci. 24 (6) (1982) 369–376.

8. J.-R. Lin, R.-F. Lu, W.-H. Liao, C.-C. Kuo, Effects of couple stresses and convective inertia forces in parallel circular squeeze-film plates, Ind. Lubr. Tribol. 56 (6) (2004) 318–323.

9. J.-R. Lin, C.-R. Hung, Effects of non-Newtonian couple stresses and fluid inertia on squeeze films between a long cylinder and an infinite plate, Fluid Dyn. Res. 39 (2007) 616–631.

10. J.-R. Lin, Oscillating circular squeeze films considering fluid inertia and couple stresses, Proc. IMechE, Part J: J. Eng. Tribol. 222 (8) (2008) 975–982.

11. J.-R. Lin, R.-F. Lu, M.-C. Lin, P.-Y. Wang, Squeeze film characteristics of parallel circular disks lubricated by ferrofluids with non-Newtonian couple stresses, Tribol. Int. 61 (2013) 56–61.

12. N.B. Naduvinamani, P.S. Hiremath, G. Gurubasavaraj, Short porous journal bearing with couple stress fluid, Tribol. Int. 34 (2001) 739–747.

13. N.B. Naduvinamani, P.S. Hiremath, S.T. Fathima, Squeeze film lubrication of long porous journal bearings with couple stress fluids, Ind. Lubr. Tribol. 57 (1) (2005) 12–20.

14. M. Nabhani, M. El Khlifi, B. Bou-Saïd, Non-Newtonian couple stress poroelastic squeeze film, Tribol. Int. 64 (2013) 116–127.

15. M. Nabhani, M. El Khlifi, B. Bou-Saïd, Combined non-Newtonian and viscous shear effects on porous squeeze film behavior, Tribol. Trans. 55 (4) (2012) 491–502.

16. N.M. Bujurke, D.P. Basti, R.B. Kudenatti, Surface roughness effects on squeeze film behavior in porous circular disks with couple stress fluid, Transp. Porous Media 71 (2008) 185–197.

17. J.-R. Lin, L.-M. Chu, W.-L. Li, R.-F. Lu, Combined effects of piezo-viscous dependency and non-Newtonian couple stresses in wide parallel-plate squeeze films, Tribol. Int. 44 (2011) 1598–1602.

18. K.R. Vasanth, B.N. Hanumagowda, J. Santhosh Kumar, Piezo-viscous dependency and couple stress in porous annular plates, J. Phys. Conf. Ser. 1000 (2018) 012080.

19. V. Kumar, H.B. Naganagowda, J. Santhosh Kumar, R.B. Thimmaiah, Combined effect of piezo-viscous dependency and non-Newtonian couple stresses in porous squeeze-film circular plates, J. Adv. Res. Fluid Mech. Therm. Sci. 51 (2) (2018) 158–168.

20. R. Vinutha, B.N. Hanumagowda, K.R. Vasanth, K. Ganesh Kumar, Theoretical analysis of the effect of MHD, couple stress and slip velocity on squeeze film lubrication of rough triangular plates, Int. J. Thermofluids 24 (2024) 100882.

21. R. Vinutha, B.N. Hanumagowda, K.R. Vasanth, Theoretical analysis of the effect of MHD, couple stress and slip velocity on squeeze film lubrication characteristics of long cylinder and infinite rough plate, Tribol. Int. 191 (2024) 109164.

22. B. Kashinath, A.C. Upadhya, Surface roughness effect on porous pivoted slider bearings with squeeze film formed by couple stress fluid, J. Sci. Res. 17 (2) (2025) 427–439. https://doi.org/10.3329/jsr.v17i2.75553.

23. A. Salma, B.N. Hanumagowda, C.K. Sreekala, T. Muhammad, Insight into the dynamics of couple-stress fluid through the porous medium between a curved circular plate and a rough flat plate: comparative analysis between radial and azimuthal roughness, Chin. J. Phys. 88 (2024) 991–1009.

24. J.-R. Lin, L.-M. Chu, W.-L. Liaw, L.-J. Mou, Effects of non-Newtonian couple stresses on the squeeze film characteristics between two different spheres, Proc. IMechE, Part J: J. Eng. Tribol. 222 (2008) 1–10.

25. Hamrock, B. J. Fundamentals of fluid film lubrication. (1994). McGraw-Hill.

26. Pinkus, O. and Sternlicht, B. Theory of hydrodynamic lubrication,(1961) (McGraw-Hill, NewYork).

Divya R.,

Department of Mathematics, Nitte Meenakshi Institute of Technology (NMIT), Bengaluru, Nitte (Deemed to be University), India.

Department of Mathematics, K. S. School of Engineering and Management, Bengaluru 560109, Karnataka, India.

Visvesvaraya Technological University, Belagavi, Karnataka, India.

E-mail address: divya.rajathadri@gmail.com,

and

Sreekala C. K.,

Department of Mathematics,

Nitte Meenakshi Institute of Technology (NMIT), Bengaluru, Nitte (Deemed to be University), India.

E-mail address: sreekalarajeesh@gmail.com

and

Hanumagowda B. N.
Department of Mathematics,
GM University, Davangere 577006, Karnataka, India
E-mail address: hanumagowda123@rediffmail.com

and

Pramod S.,
Department of Mathematics,
Nitte Meenakshi Institute of Technology (NMIT), Bengaluru, Nitte (Deemed to be University), India.
E-mail address: praup.s@gmail.com